

# Comparison and Evaluation of the Thermooxidative Stability of Medical Natural Rubber Latex Products Prepared with a Sulfur Vulcanization System and a Peroxide Vulcanization System

Mei Chen,<sup>1</sup> Ning-Jian Ao,<sup>2</sup> Bei-Long Zhang,<sup>1</sup> Chun-Mei Den,<sup>3</sup> Hong-Lian Qian,<sup>1</sup> Hui-Ling Zhou<sup>1</sup>

<sup>1</sup>Key Laboratory of Natural Rubber Processing, Ministry of Agriculture, People's Republic of China, South China Tropical Agricultural Product Processing Research Institute, P.O. Box 318, Zhanjiang 524001, Guangdong, People's Republic of China

<sup>2</sup>Institute of Biomedical Engineering, Jinan University, Guangzhou 510632, Guangdong, People's Republic of China

<sup>3</sup>Institute of Science, Zhanjiang Ocean University, Zhanjiang 524088, People's Republic of China

Received 8 July 2004; accepted 7 December 2005

DOI 10.1002/app.22047

Published online in Wiley InterScience (www.interscience.wiley.com).

**ABSTRACT:** This article deals with our study of the thermooxidative degradation of medical natural rubber latex tubes prepared with sulfur-prevulcanized latex (sample I) and peroxide-prevulcanized latex (sample II) in a dynamic air atmosphere by the use of the thermogravimetry/differential thermogravimetry method as well as the evaluation of the thermooxidative stability of these two samples. The test results showed that an oxygen-absorption mass-gain process occurred after a slight mass loss; the mass-gain rate decreased with an increase in the temperature rising rate ( $\beta$ ), and this was more prominent in sample II than in sample I. The maximum mass-gain rate of sample II was 1.43% when  $\beta$  was 5°C/min, which was 5.02 times that of sample I; the thermooxidative stability of sample II was also lower than that of sample I. Because the oxygen absorption of sample II clearly caused serious oxidation, the balanced initial temperature, the temperature of the balanced degradation peak, and the balanced final temperature of sample II in the first reaction stage were obviously lower than those of sample I. The apparent activation energy ( $E_o = 143.6$  kJ/mol) of sample I was significantly higher than that of sample II, and the

stability of sample I was also higher than that of sample II. The temperature of the balanced degradation peak of sample II in the second reaction stage was higher than that of sample I, and  $E_o$  (154.0 kJ/mol) of sample II was significantly higher than that of sample I; the stability of sample II was also higher. Thermogravimetry curves of the two samples at various  $\beta$  values intercrossed each other, and the temperature at the crosspoint and the degradation rate increased linearly as  $\beta$  increased. On the temperature segment from the initial temperature to the crosspoint, the degradation rate of sample II was higher than that of sample I when the temperature of the two samples was the same, but on the segment from the crosspoint to the final temperature, the degradation rate of sample II was lower than that of sample I when the temperature of the two samples was the same. The degradation rate of the samples at 600°C was 99.2–99.5%. © 2005 Wiley Periodicals, Inc. *J Appl Polym Sci* 98: 591–597, 2005

**Key words:** degradation; rubber; stabilization; thermogravimetric analysis (TGA); vulcanization

## INTRODUCTION

Natural rubber (NR) latex possesses no toxicity, and its products have excellent mechanical and hand-feel properties, so it has become one of the main raw materials for manufacturing medical surgery instruments (e.g., various kinds of tubes and gloves) and tools that come into contact with food. Because NR latex can be vulcanized with a sulfur vulcanization

system at a lower temperature, sulfur vulcanization is still the main and common system used for manufacturing NR latex products. Therefore, a large number of reports concerning this system have been published.<sup>1–3</sup> The accelerators used in this system contain nitrosamines or materials that can form nitrosamines. These materials can induce the formation of cancer, so they constitute a potential danger to human safety and health. Instead, the accelerators do not need be used when peroxide-prevulcanized latex (PPVL) is applied, and the latex can also be vulcanized at a lower temperature; thus, the nitrosamine problem can be avoided. In that case, extensive attention has been paid to this process,<sup>4,5</sup> but no report has been published on the preparation of rubber latex products with PPVL or on the thermooxidative degradation of these products.

Correspondence to: M. Chen (chgdzjcm@yahoo.com.cn).

Contract grant sponsor: National Science Foundation of China; contract grant number: 50063002.

Contract grant sponsor: S & T Foundation (Key Laboratory of Natural Rubber Processing, Ministry of Agriculture); contract grant number: 504067.

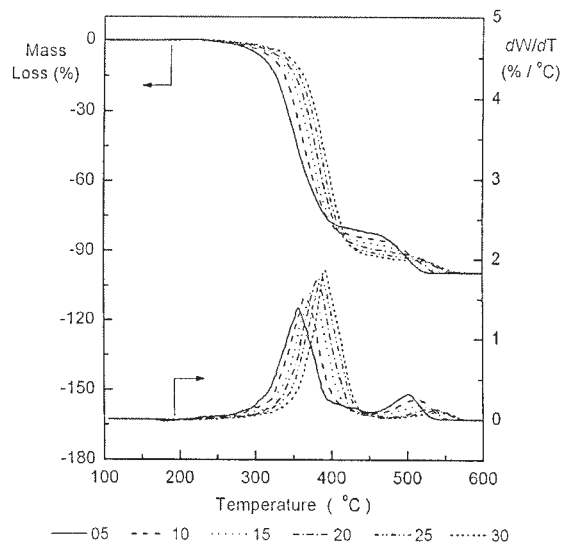


Figure 1 TG-DTG curves of sample I (100–600°C).

This article describes the thermooxidative degradation during the preparation of medical NR latex tubes with sulfur-vulcanized latex and PPVL with the thermogravimetry/differential thermogravimetry (TG-DTG) method and compares and evaluates their thermooxidative stability. We think this study will play a positive role in spreading the application of PPVL to manufacturing medical rubber latex products.

## EXPERIMENTAL

### Raw materials

The NR latex concentrate was supplied by Zhanjiang Medical Latex Product Factory. The chemical materials needed for the sulfur vulcanization system and the

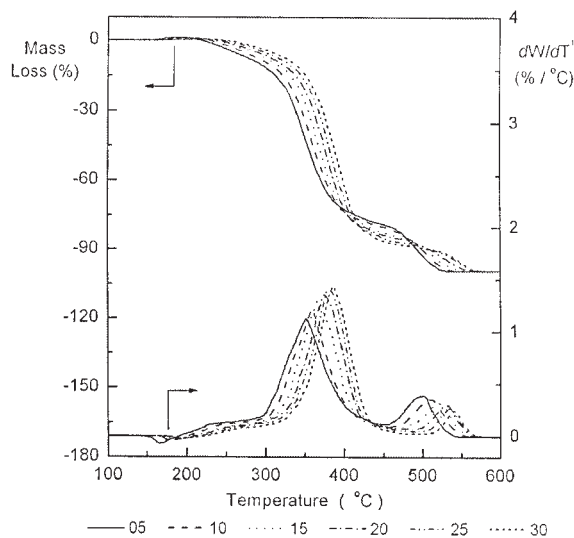


Figure 2 TG-DTG curves of sample II (100–600°C).

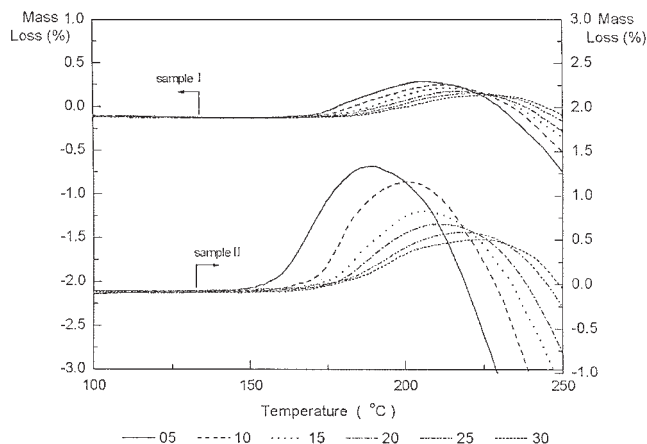


Figure 3 TG curves of samples I and II (100–250°C).

tertiary butyl peroxide (PC chemical reagent) used in the peroxide pre-vulcanization were bought from the market; the fructose (medical grade) was supplied by Zhanjiang Fructose Factory.

### Preparation of the test samples

#### Preparation of the sulfur-prevulcanized latex

The ingredients used for preparing the sulfur-prevulcanized latex were as follows (*m/m* ratio, or mass ratio): NR latex (based on dry rubber; 100), sulfur (0.8), tetramethyl thiuram disulfide (1.2), dibenzothiazole disulfide (0.5), and  $\text{ZnCO}_3$  (0.8). The prevulcanization was performed at 50°C for 45 min (chloroform grade:<sup>6</sup> 2 middle to 2 end).

#### Preparation of PPVL

The ingredients used for preparing PPVL were as follows (*m/m* ratio): NR latex (based on dry rubber; 100), tertiary butyl peroxide (0.8), fructose (1.0), and  $\text{Fe}^{3+}$  ( $4 \times 10^{-4}$ ). The tertiary butyl peroxide, fructose, and  $\text{Fe}^{3+}$  were added to the latex at the same time at 70°C; the vulcanization reaction time was 3.5 h. The swelling index (*Q*) of the PPVL film used in this experiment was 5.9. *Q* was calculated according to the following equation:

$$Q = (m_2 - m_1)/m_1 \quad (1)$$

where  $m_2$  is the mass of the vulcanized rubber film after swelling in the solvent and  $m_1$  is the mass of the vulcanized rubber film before swelling in the solvent.

The investigation carried out by Ma'zam et al.<sup>7</sup> showed that, if we applied *Q* to indicate the degree of crosslinking during the vulcanization of the PPVL film, the tensile strength of the PPVL film would reach its optimum value when *Q* was about 6.

TABLE I  
Mass-gain Peak Temperature and Mass-gain Rate of the Test Samples

|                                                   | $\beta$ ( $^{\circ}\text{C}/\text{min}$ ) |       |       |       |       |       |
|---------------------------------------------------|-------------------------------------------|-------|-------|-------|-------|-------|
|                                                   | 5                                         | 10    | 15    | 20    | 25    | 30    |
| Sample I                                          |                                           |       |       |       |       |       |
| Mass-gain peak temperature ( $^{\circ}\text{C}$ ) | 205.4                                     | 209.7 | 213.3 | 216.8 | 220.4 | 227.5 |
| Mass-gain rate (%)                                | 0.285                                     | 0.246 | 0.213 | 0.176 | 0.155 | 0.132 |
| Sample II                                         |                                           |       |       |       |       |       |
| Mass-gain peak temperature ( $^{\circ}\text{C}$ ) | 187.9                                     | 200.7 | 206.1 | 209.7 | 218.7 | 224.0 |
| Mass-gain rate (%)                                | 1.43                                      | 1.16  | 0.822 | 0.677 | 0.585 | 0.501 |

### Preparation of the rubber latex tube samples

The appropriate heat sensitizer was added to the sulfur-prevulcanized latex and PPVL, respectively. The NR latex tubes prepared with the sulfur-prevulcanized latex (sample I) and PPVL (sample II) were produced by a heat-sensitive extrusion method; the extrusion temperature was 85–90 $^{\circ}\text{C}$ .

The samples were dried in hot air (70 $^{\circ}\text{C}$ ); after that, sample I was vulcanized further in hot air (90 $^{\circ}\text{C}$  for 6 h).

### Apparatus and test method

A Seiko (Tokyo, Japan) TG-DTA 320 thermoanalyzer was used to analyze samples I and II. The mass of each test sample was about 10 mg with precision of 0.001 mg. The temperature rising rates ( $\beta$ ) were 5, 10, 15, 20, 25, and 30 $^{\circ}\text{C}/\text{min}$ . The flow rate of air was 50 mL/min.

## RESULTS AND DISCUSSION

### Thermooxidative degradation

Reaction process of thermooxidative degradation

Figures 1 and 2 present the TG–DTG curves (100–600 $^{\circ}\text{C}$ ) of samples I and II, respectively, in an air

atmosphere with  $\beta$  values of 5, 10, 15, 20, 25, and 30 $^{\circ}\text{C}/\text{min}$ . Two stages clearly appear on the thermogravimetry (TG) curves during the thermooxidative degradation of the test samples, and two corresponding peaks also appear on the differential thermogravimetry (DTG) curves; this indicates that the thermooxidative degradation reaction is a two-stage reaction.<sup>8,9</sup>The first weight-loss stage of sample I occurs at 208–425 $^{\circ}\text{C}$ , and that of sample II occurs at 190–423 $^{\circ}\text{C}$ ; the second weight-loss stage of sample I occurs at 425 to 569 $^{\circ}\text{C}$ , and that of sample II occurs at 423 to 570 $^{\circ}\text{C}$ . The features of the TG–DTG curves of the two samples are similar, and the features of the TG or DTG curves for various values of  $\beta$  are similar also. The TG and DTG curves shift to the high-temperature side as  $\beta$  increases.

Figure 3 shows the TG curves (100–250 $^{\circ}\text{C}$ ) of samples I and II with the aforementioned six different  $\beta$  values in a hot air atmosphere. A mass-gain process happens after a slight mass loss on the TG curve, and the TG curves shift toward the high-temperature side with an increase in  $\beta$  during the mass-gain period. The mass gain is more obvious in sample II than that in sample I. An obvious mass-loss degradation appears again immediately after the mass gain.

The mass-gain peak temperature and mass-gain rate of the two samples are listed in Table I. The largest peak temperatures of samples I and II rise with an

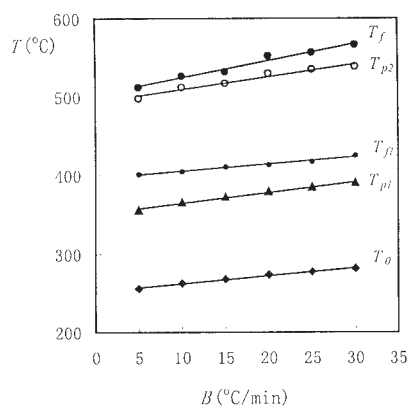


Figure 4 Relation between  $\beta$  and  $T$  of sample I.

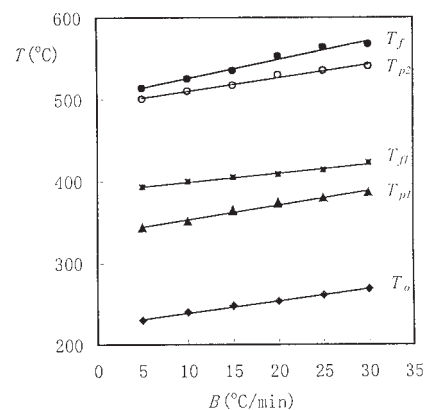


Figure 5 Relation between  $\beta$  and  $T$  of sample II.

TABLE II  
Balanced Degradation Temperatures (°C)  
of the Test Samples

| Sample | $T_0^0$ | $T_{p1}^0$ | $T_{f1}^0$ | $T_{p2}^0$ | $T_f^0$ |
|--------|---------|------------|------------|------------|---------|
| I      | 252.1   | 351.2      | 396.2      | 491.9      | 502.9   |
| II     | 223.5   | 335.8      | 387.7      | 493.7      | 503.1   |

increase in  $\beta$ , but the mass-gain rate decreases. The increase in the largest peak temperature is correlated linearly with a decrease in the mass-gain rate. The correlation coefficients ( $r$ ) of samples I and II are 0.9528 and 0.9545, respectively.

Table I also shows that the mass-gain peak temperatures of  $\beta$  in sample II are lower than those in sample I, but the maximum mass-gain rates are obviously higher. The largest rate is 5.02 times higher when  $\beta$  is 5°C/min, and the lowest rate is 3.79 times higher when  $\beta$  is 30°C/min. The mass gain of the test sample is due to the oxygen absorption of rubber. There are natural antiagers in the NR latex, and they have a positive effect on the age resistance of rubber; because of the breakdown of the natural antiagers in the NR latex during peroxide prevulcanization in sample II,<sup>10</sup> the protective action of the antiager to rubber hydrocarbon is lost, and so under the action of heat and oxygen, the formation of free radicals is accelerated, and these radicals are oxidized into hydroperoxide. This causes an earlier appearance of the mass-gain peak temperatures and makes the mass-gain rates more obvious, and the thermooxidative stability of sample II is also lower than that of sample I.

#### Relation between $\beta$ and the degradation temperature ( $T$ )

Figures 1 and 2 show that the mass gain of samples I and II occurs before the first reaction stage (i.e., the main degradation stage), so if we try to determine the initial degradation temperature ( $T_0$ ) by extrapolation with the double-tangent method, an error will occur. Therefore, the temperature of the test sample at 1% degradation has been applied to determine  $T_0$ . The final degradation temperature ( $T_{f1}$ ) in the first stage and the last final degradation temperature ( $T_f$ ) have been obtained by extrapolation with the double-tangent method from TG curves in Figures 1 and 2,

respectively. The degradation peak temperatures  $T_{p1}$  and  $T_{p2}$  have been obtained from the DTG curves in Figures 1 and 2, respectively.

The relations between  $\beta$  and the degradation temperature ( $T$ ) of samples I and II are presented in Figures 4 and 5, respectively.

The correlation equations can be obtained from Figures 4 and 5 as follows:

$$\text{Sample I: } T_0 = 1.014\beta + 252.1, T_{p1} = 1.354\beta + 351.2, \\ T_{f1} = 0.917\beta + 396.2, T_{p2} = 1.673\beta + 491.9, \text{ and} \\ T_f = 2.187\beta + 502.9.$$

$$\text{Sample II: } T_0 = 1.515\beta + 223.5, T_{p1} = 1.773\beta \\ + 335.8, T_{f1} = 1.102\beta + 387.7, T_{p2} = 1.650\beta \\ + 493.7, \text{ and } T_f = 2.316\beta + 503.1.$$

Figures 4 and 5 show that  $T$  rises linearly with an increase in  $\beta$  in both samples I and II. The width of the degradation peak during the first reaction stage of sample I ( $T_{f1} - T_0$ ) is  $-0.097\beta + 144.1^\circ\text{C}$ , and that of sample II is  $-0.413\beta + 164.2^\circ\text{C}$ ; this indicates that the width of the degradation peak of samples I and II decreases with an increase in  $\beta$ .

For  $\beta = 0$ , the balanced degradation temperatures of the thermooxidative degradation of the two samples are listed in Table II. Table II shows that the balanced degradation temperatures of sample I in the first stage [balanced initial temperature ( $T_0^0$ ), temperature of the balanced degradation peak ( $T_{p1}^0$ ), and balanced final temperature ( $T_{f1}^0$ )] are higher than those of sample II, but the temperature of the balanced degradation peak in the second stage ( $T_{p2}^0$ ) is lower than that of sample II, and the balanced last final degradation temperature ( $T_f^0$ ) is slightly lower than that of sample II.

#### Effect of $\beta$ on the degradation rate ( $C$ )

The maximum thermooxidative degradation rate ( $C_p$ ) at different  $\beta$  values in the thermooxidative degradation reaction have been obtained from TG-DTG curves and are listed in Tables III and IV. Table III shows that  $C_{p1}$  of the two test samples in the first reaction stage rises with an increase in  $\beta$ , and this indicates that the reaction of rubber to the heat hysteresis effect is more significant in the first stage. Table III also shows that the average  $C_{p1}$  value of sample I is lower than that of sample II; Table IV shows that the

TABLE III  
Relation Between  $C_p$  and  $\beta$  of the Test Samples in the First Reaction Stage

|                        | $\beta$ (°C/min) |      |      |      |      |      | Average |
|------------------------|------------------|------|------|------|------|------|---------|
|                        | 5                | 10   | 15   | 20   | 25   | 30   |         |
| Sample I $C_{p1}$ (%)  | 42.2             | 43.1 | 43.7 | 44.0 | 44.2 | 45.6 | 43.8    |
| Sample II $C_{p1}$ (%) | 42.6             | 43.7 | 43.9 | 44.1 | 44.2 | 46.4 | 44.2    |

TABLE IV  
Relation Between  $C_p$  and  $\beta$  of the Test Samples in the Second Reaction Stage

|                        | $\beta$ (°C/min) |      |      |      |      |      | Average |
|------------------------|------------------|------|------|------|------|------|---------|
|                        | 5                | 10   | 15   | 20   | 25   | 30   |         |
| Sample I $C_{p2}$ (%)  | 93.9             | 93.9 | 94.5 | 95.1 | 95.5 | 95.8 | 94.8    |
| Sample II $C_{p2}$ (%) | 93.5             | 93.9 | 94.0 | 94.2 | 93.7 | 93.5 | 93.8    |

average  $C_{p2}$  value of sample II is lower than that of sample I.

Figure 6 presents a diagram of TG curves of samples I and II with a single Y coordinate at various  $\beta$  values and shows that the TG curves of the two samples intercross each other. On the temperature segment from  $T_o$  to the crosspoint,  $C$  of sample II is higher than that of sample I at the same temperature, but on the segment from the crosspoint to  $T_f$ ,  $C$  of sample II is lower than that of sample I at the same temperature (so that the curves are clearer, only the adjacent parts of the crosspoints are shown in the diagram). Figure 6 and Table V show that the temperatures at the crosspoints of the curves and  $C$  linearly rise with an increase in  $\beta$ .

The bond energy of  $-C-$  is higher than that of  $-S-$  or  $-S-S-$ , so the thermooxidative stability of sample II is higher than that of sample I at a higher temperature. Our previous work<sup>11,12</sup> has shown that from the FTIR curve of PPVL film, it can be seen that the absorption peak of  $2965\text{ cm}^{-1}$  (the antisymmetrical vibration absorption of the saturated hydrocarbon  $-CH_3$ ) and the absorption peak of  $2868\text{ cm}^{-1}$  (the symmetrical vibration absorption of the saturated hydrocarbon  $-CH_3$ )<sup>13</sup> weaken gradually with an extension of the aging time; this indicates that  $C-C$  crosslinkages are formed in rubber molecules during peroxide vulcanization, and this makes some of the NR molecules form saturated hydrocarbon. This is in conformity with Loan's<sup>14</sup> viewpoint.

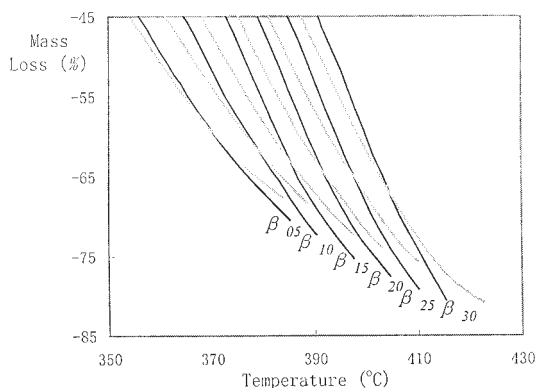


Figure 6 Intercrossing of TG curves of samples I (black line) and II (gray line).

Tables II–IV and Figure 6 indicate that the thermooxidative stability of sample I in the first reaction stage is higher than that of sample II, and the thermooxidative stability of sample II in the second reaction stage is higher than that of sample I.

The residues of the two samples remaining at  $600^\circ\text{C}$  amount to 0.5–0.8%.

### Kinetics of the thermooxidative degradation reaction of the test samples

#### Data processing

The TG data of the test samples have been processed with the method of integration according to the Coats–Redfern<sup>15</sup> equation to determine the corresponding data of the reaction kinetics of the test samples. After the mathematical processing of the reaction kinetics equation

$$da/dt = k(1 - \alpha)^{11} \quad (2)$$

and the Arrhenius equation

$$k = Ae^{-E/RT} \quad (3)$$

the following equation has been obtained:

$$\ln\{[1 - (1 - \alpha)^{1-n}]/[T^2(1 - n)]\} = \ln\{[1 - 2RT/E)AR/\beta E] - E/RT (n \neq 1) \quad (4)$$

where  $n$  is the reaction order,  $\alpha$  is the reaction degree,  $T$  is the absolute temperature,  $E$  is the activation energy of reaction,  $R$  is the gas constant, and  $A$  is the frequency factor. When  $n$  is not equal to 1, a straight line can be obtained from the diagram with  $\ln\{[1 - (1 -$

TABLE V  
Temperature and Thermooxidative Degradation Rate of the Crosspoints ( $T$ ) on the TG Curves of Samples (C) I and II

|          | $\beta$ (°C/min) |       |       |       |       |       |
|----------|------------------|-------|-------|-------|-------|-------|
|          | 5                | 10    | 15    | 20    | 25    | 30    |
| $T$ (°C) | 370.1            | 379.1 | 385.8 | 392.3 | 398.2 | 405.1 |
| $C$ (%)  | 59.3             | 61.5  | 63.4  | 64.7  | 65.5  | 67.6  |



TABLE VI  
Parameters of the Thermooxidative Degradation Kinetics of the Test Samples in the First Reaction Stage

|                     | $\beta$ (°C/min) |        |        |        |         |         |
|---------------------|------------------|--------|--------|--------|---------|---------|
|                     | 5                | 10     | 15     | 20     | 25      | 30      |
| Sample I            |                  |        |        |        |         |         |
| $n$                 | 1.7              | 1.7    | 1.7    | 1.7    | 1.7     | 1.7     |
| $E$<br>(kJ/mol)     | 148.4            | 166.1  | 175.2  | 181.4  | 193.2   | 196.2   |
| $A \times 10^{-12}$ | 0.43             | 17.22  | 88.45  | 270.69 | 2342.30 | 3655.84 |
| $r$                 | 0.9990           | 0.9997 | 0.9999 | 0.9998 | 0.9996  | 0.9996  |
| Sample II           |                  |        |        |        |         |         |
| $n$                 | 1.7              | 1.7    | 1.7    | 1.7    | 1.7     | 1.7     |
| $E$<br>(kJ/mol)     | 116.5            | 120.0  | 135.7  | 144.9  | 152.8   | 154.9   |
| $A \times 10^{-10}$ | 0.07             | 0.22   | 5.34   | 31.52  | 138.19  | 187.84  |
| $r$                 | 0.9997           | 0.9995 | 0.9996 | 0.9997 | 0.9995  | 0.9992  |

$-\alpha^{1-n}]/[T^2(1-n)]$  and  $1/T$  as coordinates; the intercept of the line is  $\ln[(1-2RT/E)AR/\beta E]$ . When the maximum  $r$  value is obtained by use of the least-square fit method with a different  $n$  value, then  $n$  is the reaction order sought and the corresponding  $E$  value is the reaction activation energy sought.

#### Kinetics of the thermooxidative degradation reaction

The thermooxidative data of the test samples have been processed with the Coats-Redfern equation. The parameters of the thermooxidative degradation kinetics are listed in Tables VI and VII. Table VI shows that the thermooxidative degradation reaction order ( $n$ ) of samples I and II in the first stage is 1.7, and it is not affected by  $\beta$ . Table VI also shows that  $E$  of the two samples increases with an increase in  $\beta$ ; the linear regression is carried out with the least-square method to determine  $E_o$  at  $\beta = 0^\circ\text{C}/\text{min}$ . The  $E_o$  values of samples I and II are 143.6 and 107.5 kJ/mol, respectively;  $E$  at different  $\beta$  values and  $E_o$  of sample I are higher than those of sample II, and this indicates that the thermooxidative stability of sample I is higher than that of sample II in the first reaction stage.  $A$  of the two samples increases almost with geometric pro-

gression as  $\beta$  increases. The maximum  $r$  values of the two samples are greater than 0.999.

Table VII shows that  $n$  of samples I and II in the second reaction stage varies with  $\beta$ , but no correlation exists between these two factors. The  $E_o$  values of samples I and II are 131.1 and 154.0 kJ/mol, respectively, and  $E$  at different  $\beta$  values and  $E_o$  of sample II are higher than those of sample I; this indicates that the thermooxidative stability of sample II is higher than that of sample I in the second reaction stage.

## CONCLUSIONS

A mass gain occurs after a slight mass loss on the TG curves of the two samples, and the mass gain is more obvious in sample II than in sample I. The maximum mass-gain rate of sample II is 1.43% when  $\beta$  is  $5^\circ\text{C}/\text{min}$ , which is 5.02 times that of sample I; the thermooxidative stability of sample II is also lower than that of sample I.

The thermooxidative degradation of the two samples is a two-stage reaction.  $T_o^0$ ,  $T_{P1}^0$ ,  $T_{f1}^0$ , and  $E_o$  of sample I in the first reaction stage are higher than those of sample II; the stability of sample I is also higher than that of sample II.  $T_{P2}^0$  and  $E_o$  of sample I in the second reaction stage are lower than those of sample II; the stability of sample I is also lower than that of sample II.

The two corresponding TG curves of the two samples at various  $\beta$  values intercross each other. On the temperature segment from  $T_o$  to the crosspoint,  $C$  of sample II is higher than that of sample I when the temperature of the two samples is the same, but on the segment from the crosspoint to  $T_f$ ,  $C$  of sample II is lower than that of sample I when the temperature of the two samples is the same.

## References

1. Van Gils, G. E. *Rubber Chem Technol* 1977, 50, 141.
2. Chen, M.; Ao, N.-J.; Bian, J.; Zhou H.-L.; Qian H.-L. *China Rubber Ind* 2003, 50, 418.

TABLE VII  
Part Parameters of the Thermooxidative Degradation Kinetics of the Test Samples in the Second Reaction Stage

|              | $\beta$ (°C/min) |       |       |       |       |       |
|--------------|------------------|-------|-------|-------|-------|-------|
|              | 5                | 10    | 15    | 20    | 25    | 30    |
| Sample I     |                  |       |       |       |       |       |
| $n$          | 1.7              | 1.7   | 1.8   | 1.7   | 1.8   | 1.9   |
| $E$ (kJ/mol) | 140.8            | 142.6 | 146.9 | 158.0 | 166.2 | 170.5 |
| Sample II    |                  |       |       |       |       |       |
| $n$          | 1.6              | 1.6   | 1.7   | 1.7   | 1.8   | 1.7   |
| $E$ (kJ/mol) | 159.0            | 171.9 | 177.3 | 187.4 | 194.5 | 198.3 |

3. Cai, H.-H.; Li, S.-D.; Tian, G.-R.; Wang, H.-B.; Wang, J.-H. *J Appl Polym Sci* 2003, 87, 982.
4. Davies, R. T.; Gazeley, K. F. *Malaysian J Nat Rubber Res* 1993, 8, 176.
5. Zhang, B.-L.; Chen, M.; Deng, W.-Y.; Liu, H.-L. *China Polym Mater Sci Eng* 2003, 19, 191.
6. Zhao, G.-X.; Wang, D.-J.; Wei, B.-Z. *Handbook of Rubber Industry*, 7th ed.; Chemical Industrial: Beijing, 1990; p 405.
7. Ma'zam, M. D. S.; Pendle, T. D.; Blackley, D. C. *Malaysian J Nat Rubber Res* 1991, 6, 158.
8. Zhong, J.-P.; Li, S.-D.; Yu, H.-P.; Wei, Y.-C.; Pen, Z.; Qu, J.-L.; Guo, C.-K. *J Appl Polym Sci* 2001, 81, 1305.
9. Li, S.-D.; Cheung, M.-K.; Zhong, J.-P.; Yu, H.-P. *J Appl Polym Sci* 2001, 82, 2590.
10. Ma'zam, M. D. S.; Pendle, T. D.; Blackley, D. C. *Malaysian J Nat Rubber Res* 1990, 5, 27.
11. Chen, M.; Zhang, B.-L.; Peng, Z.; Liu, H.-L. *China J Funct Mater* 2001, 32, 1345.
12. Zhang, B.-L.; Chen, M.; Ao, N.-J.; Deng, W.-Y. *J Appl Polym Sci* 2004, 92, 3196.
13. Dong, Q.-N. *IR Spectrographic Methods*; Chemical Industry: Beijing, 1974; p 104.
14. Loan, L. D. *Rubber Chem Technol* 1967, 40, 149.
15. Coats, A. W.; Redfern, J. P. *J Nat* 1964, 201, 68.